Synthesis and Reactivity of Tethered η^1:η^6-(Phosphinoarene)ruthenium Dichlorides

Bruno Therrien,[†] Thomas R. Ward,*[,†] Melanie Pilkington,[‡] Christina Hoffmann,[‡] François Gilardoni,[§] and Jacques Weber[§]

Department of Chemistry and Biochemistry and Laboratory of Chemical and Mineralogical Crystallography, University of Berne, Freiestrasse 3, CH-3012 Berne, Switzerland, and Department of Physical Chemistry, University of Geneva, 30 Quai E. Ansermet, CH-1211 Geneva 4, Switzerland

Received August 18, 1997

The coordination properties of *ortho*- and *meta*-substituted [(2-diphenylphosphanylethyl)-phenyl]methanol **4a** and **4b** toward ruthenium(II) have been investigated. To ensure coordination of both the arene and the tethered phosphine, the labile ruthenium arene dimer $[RuCl_2(EtO_2CC_6H_5)]_2$ (**7**) was synthesized and structurally characterized. Both the *ortho* and *meta* isomers [Ru(**4a**)Cl_2] (**9a**) and [Ru(**4b**)Cl_2] (**9b**) were characterized by X-ray crystallography. The lack of reactivity of the benzylic alcohol functionality in complexes **9a** and **9b** toward various P and C electrophiles is rationalized with extended Hückel calculations.

Introduction

Although the possibility of metal-based chirality was demonstrated nearly 100 years ago by A. Werner,[1] H. Brunner gave it a new impetus as he initiated a systematic study of pseudotetrahedral chiral three-legged piano-stool complexes.[2,3] Compounds of the type $[CpML^1L^2L^3]$ (Cp = cyclopentadienyl) are chiral at the metal and can be resolved in many cases if an element of chirality is introduced either on one of the ligands L, on the Cp ring, or as a counterion. After diastereomer separation, the enantiopure resolving agent can be removed, affording a chiral-at-metal compound.

Over the years, a number of groups have studied such enantiopure complexes together with applications in organic transformations. Several elegant examples of the latter come from the groups of Brunner,[3−5] Davies,[6,7] Faller,[8−14] and Gladysz.[15] To the best of our knowledge, however, chiral-at-metal compounds have only found stoichiometric (and not catalytic) applications in organic chemistry.

Recently, organometallic compounds with a d^6 electron count have been used as Lewis-acid catalysts in C−C bond-forming reactions, e.g., in Diels−Alder and Mukaiyama reactions.[16−23] The prospective of using a chiral-at-metal piano-stool complex as a catalyst for such enantioselective transformations is very appealing, but it is imperative to ensure configurational stability of the catalyst, as racemization of the latter would have a dramatic effect on the enantiomeric excess of the resulting products.

We have recently reported a theoretical study on the configurational stability of coordinatively unsaturated two-legged piano-stool complexes of the type $[(\eta^n\text{-}C_nH_n)\text{-}ML_1L_2]$, $\eta = 5-7$. Although these may have pyramidal (and thus chiral-at-metal) ground-state geometries, the computed inversion barriers are low, i.e., <15 kcal·mol^{-1}.[24]

In order to study the role of chirality at the metal in enantioselective catalysis, we set out to synthesize complexes incorporating bifunctionalized arenes, acting

[†] Department of Chemistry and Biochemistry, Universityof Berne.
[‡] Laboratory of Chemical and Mineralogical Crystallography, University of Berne.
[§] University of Geneva.

(1) Werner, A. *Ber. Dtsch. Chem. Ges.* **1911**, *44*, 1887.
(2) Brunner, H. *Angew. Chem., Int. Ed. Engl.* **1969**, *8*, 382; *Angew. Chem.* **1969**, *81*, 395.
(3) Brunner, H. *Adv. Organomet. Chem.* **1980**, *18*, 151.
(4) Brunner, H.; Aclasis, J.; Langer, M.; Steger, W. *Angew. Chem., Int. Ed. Engl.* **1974**, *13*, 810; *Angew. Chem.* **1974**, *81*, 864.
(5) Brunner, H.; Fisch, K.; Jones, P. G.; Salbeck, J. *Angew. Chem., Int. Ed. Engl.* **1989**, *28*, 1521; *Angew. Chem.* **1989**, *101*, 1558.
(6) Davies, S. G. *Pure Appl. Chem.* **1988**, *60*, 13.
(7) Davies, S. G. *Aldrichimica Acta* **1990**, *23*, 31.
(8) Faller, J. W.; Lambert, C.; Mazzieri, M. R. *J. Organomet. Chem.* **1990**, *383*, 161.
(9) Faller, J. W.; Linebarrier, D. L. *J. Am. Chem. Soc.* **1989**, *111*, 1937.
(10) Faller, J. W.; Linebarrier, D. L. *Organometallics* **1990**, *9*, 3182.
(11) Faller, J. W.; Nguyen, J. T.; Ellis, W.; Mazzieri, M. R. *Organometallics* **1993**, *12*, 1434.
(12) Faller, J. W.; Ma, Y. *Organometallics* **1992**, *11*, 2726.
(13) Faller, J. W.; Mazzieri, M. R.; Nguyen, J. T.; Parr, J.; Tokunaga, M. *Pure Appl. Chem.* **1994**, *66*, 1463.
(14) Schilling, B. E. R.; Hoffmann, R.; Faller, J. W. *J. Am. Chem. Soc.* **1979**, *101*, 592.
(15) Gladysz, J. A.; Boone, B. J. *Angew. Chem., Int. Ed. Engl.* **1997**, *36*, 550; *Angew. Chem.* **1997**, *109*, 566.
(16) Bonnesen, P. V.; Puckett, C. L.; Honeychuck, R. V.; Hersh, W. H. *J. Am. Chem. Soc.* **1989**, *111*, 6070.
(17) Bach, T.; Fox, D. N. A.; Reetz, M. T. *J. Chem. Soc., Chem. Commun.* **1992**, 1634.
(18) Kündig, E. P.; Bourdin, B.; Bernardinelli, G. *Angew. Chem., Int. Ed. Engl.* **1994**, *33*, 1856; *Angew. Chem.* **1994**, *106*, 1931.
(19) Hollis, T. K.; Odenkirk, W.; Robinson, N. P.; Whelan, J.; Bosnich, B. *Tetrahedron* **1993**, *49*, 5415.
(20) Odenkirk, W.; Whelan, J.; Bosnich, B. *Tetrahedron Lett.* **1992**, *39*, 5729.
(21) Odenkirk, W.; Rheingold, A. L.; Bosnich, B. *J. Am. Chem. Soc.* **1992**, 6392.
(22) Faller, J. W.; Smart, C. J. *Tetrahedron Lett.* **1989**, *30*, 1189.
(23) Faller, J. W.; Ma, Y.; Smart, C. J.; DiVerdi, M. J. *J. Organomet. Chem.* **1991**, *420*, 237.
(24) Ward, T. R.; Schafer, O.; Daul, C.; Hofmann, P. *Organometallics* **1997**, *16*, 3207.

S0276-7333(97)00735-8 CCC: $15.00
Publication on Web 01/08/1998

Scheme 1

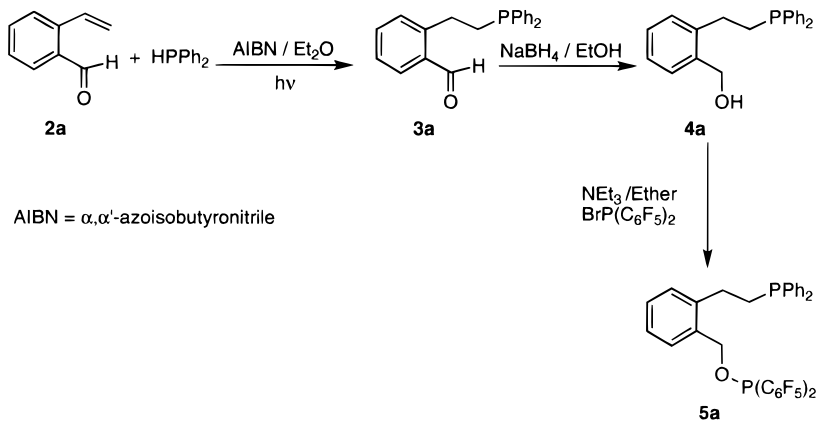

as 10-electron donors, which force pyramidalization at the metal as illustrated in **1**. In the field of early

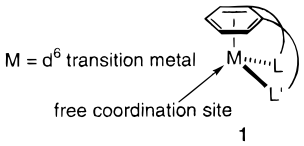

1

transition metal chemistry, tethered cyclopentadienyl ligands have recently received increasing attention, mostly in connection with stereospecific olefin polymerization.[25,26] Comparatively, tethered benzene systems have received much less attention.[27−30] We report herein the synthesis, characterization, and reactivity of arene−ruthenium complexes incorporating tethered phosphines.

Results and Discussion

Given the ultimate goal of studying the importance of electronic asymmetry in enantioselective transformations, we designed the 10-electron-donor ligand **5a** which incorporates an arene, a strong σ-donor, and a π-acceptor. This type of electronic asymmetry is responsible for the high degrees of enantioselection observed with Faller's {CpMoNOCO} as well as Gladysz's $\{CpReNOPPh_3\}^+$ Lewis-acid fragments.[14,15]

From steric considerations, the diphenylphosphine ($RPPh_2$) and perfluorodiphenylphosphinite ($R'OP(C_6F_5)_2$) donor sites can be considered as nearly equivalent. From an electronic standpoint, however, these sites differ markedly. Anchoring these two P-donors on an arene yields a potential 10-electron-donor ligand which should ensure pyramidalization of the metal upon η^6:η^1:η^1-coordination. The synthesis of phosphino phosphinite **5a** is presented in Scheme 1. Radical addition of $HPPh_2$ on vinyl aldehyde **2a** quantitatively yields **3a**, which is reduced with $NaBH_4$ to the corresponding alcohol **4a**. Functionalization of the benzylic alcohol **4a** with $BrP(C_6F_5)_2$ affords **5a** in 32% overall yield.

Ru(II) complexes incorporating the 10-electron-donor ligand **5a** should be well-suited for the activation of coordinated carbonyl moieties toward nucleophiles. Despite the presence of an electron-rich diphenylphosphine, the neutral η^6-arene, coupled with the π-acceptor properties of perfluorophosphinites,[31,32] resulting in complexes $[Ru(\eta^6{:}\eta^1{:}\eta^1\text{-}\mathbf{5a})L]^+$ (L = weakly bound ligand), are expected to display Lewis-acidic character. Attempts to coordinate phosphino phosphinite **5a** to $[RuCl_2(p\text{-cymene})]_2$[33,34] yielded complex mixtures of nearly insoluble materials. FAB MS (peaks with m/z >> 2000) and ^{31}P NMR (complex multiplets centered at 25 ppm (coordinated $RPPh_2$) and 130 ppm (coordinated $ROP(C_6F_5)_2$) revealed the presence of a polynuclear material, as one could expect for a flexible bidentate ligand, yielding a 10-membered chelate ring (without η^6-arene coordination). Heating the reaction mixture—with or without TlOTf—to obtain the thermodynamic, chelated, mononuclear complex $[Ru(\eta^6{:}\eta^1{:}\eta^1\text{-}\mathbf{5a})Cl]^+$ lead to decomposition products: the Arbuzov rearrangement product of the benzylic phosphinite ($R'CH_2OP(C_6F_5)_2$), yielding the corresponding phosphine oxide ($R'CH_2P(O)(C_6F_5)_2$), was identified by ^{31}P NMR (quintets in the region of −50 ppm).

We, thus, turned our attention to the phosphino alcohol **4a** and its coordination properties. We reasoned that the alcohol functionality could be judiciously used to resolve the enantiomers of racemic, planar chiral complex **9a** before introducing the second phosphorus tether. Reaction of **4a** with 0.5 equiv of $[Ru(\eta^6\text{-}p\text{-cymene})Cl_2]_2$ yields $[Ru(\eta^6\text{-}p\text{-cymene})(\eta^1\text{-}\mathbf{4a})Cl_2]$ (**6a**) quantitatively. All attempts to displace *p*-cymene from **6a**, either thermally or photochemically, resulted in decomposition, with only traces of **9a**. Single crystals of **6a** were submitted for X-ray analysis to determine its structure. An ORTEP plot of the molecular structure of compound **6a** is presented in Figure 1. Relevant metrical data are collected in Table 1.

It has long been known that arene-displacement reactions at Ru(II) are often low yielding.[34] We hoped,

(25) Okuda, J. *Comm. Inorg. Chem.* **1994**, *16*, 185.
(26) Shapiro, P. J.; Bunel, E.; Schaefer, W. P.; Bercaw, J. E. *Organometallics* **1990**, *9*, 867.
(27) Singewald, E. T.; Mirkin, C. A.; Levy, A. D.; Stern, C. L. *Angew. Chem., Int. Ed. Engl.* **1994**, *33*, 2473; *Angew. Chem.* **1994**, *106*, 2524.
(28) Nesmeyanov, A. N.; Krivykh, V. V.; Rubinskaya, M. I. *J. Organomet. Chem.* **1979**, *164*, 159−175.
(29) Hartshorn, C. M.; Steel, P. J. *Angew. Chem., Int. Ed. Engl.* **1996**, *35*, 2655; *Angew. Chem.* **1996**, *108*, 2818.
(30) Le Bozec, H.; Touchard, D.; Dixneuf, P. H. *Adv. Organomet. Chem.* **1989**, *29*, 163.
(31) Kündig, E. P.; Dupré, C.; Bourdin, B.; Cunningham, A. Jr.; Pons, D. *Helv. Chim. Acta* **1994**, *77*, 421.
(32) King, R. B. *Acc. Chem. Res.* **1980**, *13*, 243.
(33) Bennett, M. A.; Huang, T.-N.; Matheson, T. W.; Smith, A. K. *Inorg. Synth.* John Wiley: New York, 1982; Vol. 21, p 74.
(34) Bennett, M. A.; Smith, A. K. *J. Chem. Soc., Dalton Trans.* **1974**, 233.

Scheme 2

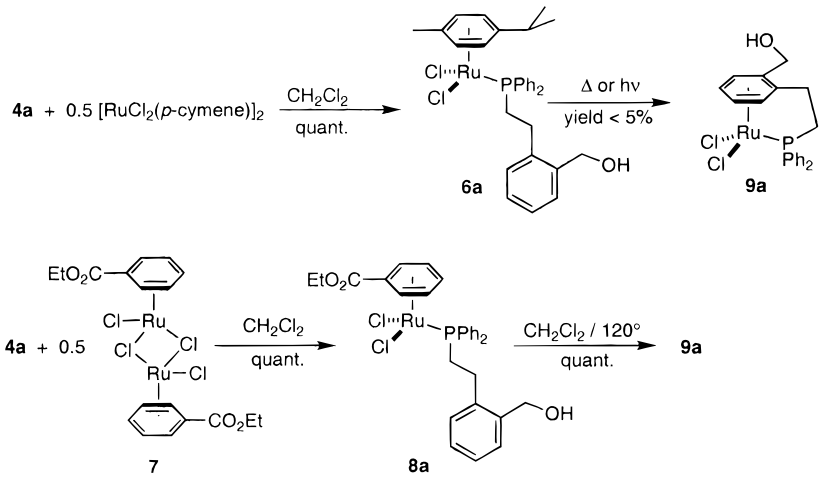

Table 1. Selected Interatomic Distances (Å), Interatomic Angles (deg) and Torsion Angles (deg) for Compound 6a[a]

Ru(1)−Cl(1)	2.428(2)	Ru(1)−C(134)	2.220(5)
Ru(1)−Cl(2)	2.423(2)	Ru(1)−C(135)	2.200(6)
Ru(1)−P(1)	2.357(2)	Ru(1)−C(136)	2.171(6)
Ru(1)−C(131)	2.208(6)	O(1)−C(109)	1.409(7)
Ru(1)−C(132)	2.228(6)	C(108)−C(109)	1.520(9)
Ru(1)−C(133)	2.244(5)	Ru(1)−centroid	1.704(7)
Cl(1)−Ru(1)−Cl(2)	87.18(6)	centroid−Ru(1)−Cl(1)	127.4(1)
Cl(1)−Ru(1)−P(1)	84.44(5)	centroid−Ru(1)−Cl(2)	125.2(1)
Cl(2)−Ru(1)−P(1)	88.00(5)	centroid−Ru(1)−P(1)	130.3(1)
P(1)−C(101)−C(102)−C(103)		180.0(4)	
O(1)−C(109)−C(108)−C(103)		−171.8(5)	
P(2)−C(201)−C(202)−C(203)		178.2(4)	
O(2)−C(209)−C(208)−C(203)		−160.7(6)	

[a] Averaged over the two independent molecules.

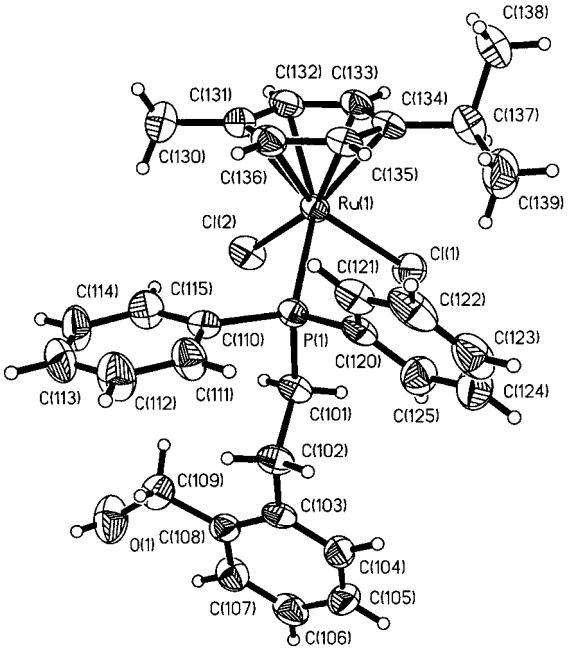

Figure 1. Molecular structure of [Ru(η^6-*p*-cymene){*o*-(C_6H_4)(CH_2OH)$CH_2CH_2PPh_2$}Cl_2] (**6a**). Thermal ellipsoids are at the 50% probability level (only one of the two independent molecules is depicted).

however, that the chelate effect may force the arene to displace the coordinated *p*-cymene in **6a**. Having failed, we sought to synthesize a more labile ruthenium arene

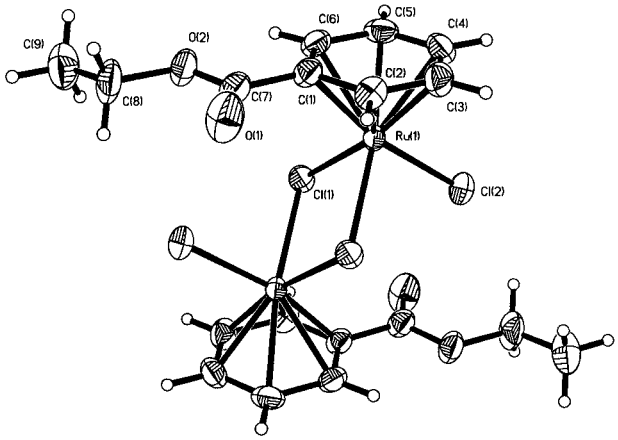

Figure 2. Molecular structure of [Ru(η^6-$C_6H_5CO_2Et$)Cl_2]$_2$ (**7**). Thermal ellipsoids are at the 50% probability level.

dimer. Since electron-poor arenes give the lowest yields in displacement reactions with [Ru(η^6-*p*-cymene)Cl_2]$_2$, we reasoned that [Ru(η^6-$C_6H_5CO_2Et$)Cl_2]$_2$ (**7**) may be a good starting material for the synthesis of **9a**, Scheme 2. Birch reduction of ethyl benzoate yielding ethyl-1,4-cyclohexadiene-3-carboxylate,[35−37] followed by reaction with $RuCl_3$ in EtOH, yields **7** in 96% yield. As dimer **7** is a promising starting material for arene-exchange reactions, its structure was elucidated by X-ray diffraction. An ORTEP plot of the molecular structure of compound **7** is presented in Figure 2. Relevant metrical data are collected in Table 2.

Treatment of dimer **7** with phosphino alcohol **4a** cleanly affords [Ru(η^6-$C_6H_5CO_2Et$)(η^1-**4a**)Cl_2] (**8a**). The intramolecular arene exchange leading to **9a** is conveniently monitored by ^{31}P NMR spectroscopy. Upon η^6:η^1-coordination of **4a**, the ^{31}P NMR signal is shifted downfield by 20 ppm (compared to **8a**). This reaction is most effectively carried out in a sealed tube in CH_2Cl_2 at 120 °C. On completion, **9a** is precipitated by the addition of hexane to the reaction mixture, yielding an orange powder. The presence of diastereotopic meth-

(35) Rabideau, P. W.; Huser, D. L.; Nyikos, S. J. *Tetrahedron Lett.* **1980**, *21*, 1401.
(36) Pertici, P.; Salvadori, P.; Biasci, A.; Vitulli, G.; Bennett, M. A.; Kane-Maguire, L. A. P. *J. Chem. Soc., Dalton Trans.* **1988**, 315.
(37) Mashima, K.; Kusano, K.-h.; Sato, N.; Matsumura, Y.-i.; Nozaki, K.; Kumobayashi, H.; Sayo, N.; Hori, Y.; Ishizaki, T.; Akutagawa, S.; Takaya, H. *J. Org. Chem.* **1994**, *59*, 3064.

Table 2. Selected Interatomic Distances (Å) and Angles (deg) for Compound 7

Ru(1)−Ru(1)#1[a]	3.718(1)	Ru(1)−C(3)	2.169(3)
Ru(1)−Cl(1)	2.4440(8)	Ru(1)−C(4)	2.164(3)
Ru(1)−Cl(2)	2.3871(9)	Ru(1)−C(5)	2.178(3)
Ru(1)−Cl(1)#1	2.4387(8)	Ru(1)−C(6)	2.160(3)
Ru(1)−C(1)	2.196(3)	Ru(1)−centroid	1.648(3)
Ru(1)−C(2)	2.158(3)		
Cl(1)−Ru(1)−Cl(2)	86.97(3)	Cl(1)−Ru(1)−Cl(1)#1	80.82(3)
centroid−Ru(1)−Cl(1)	129.7(1)	Cl(2)−Ru(1)−Cl(1)#1	87.26(3)
centroid−Ru(1)−Cl(2)	126.8(1)	Ru(1)−Cl(1)−Ru(1)#1	99.18(3)
centroid−Ru(1)−Cl(1)#1	129.6(1)		

[a] Symmetry transformations used to generate equivalent atoms: #1 $-x+1,-y,-z+1$.

Scheme 3

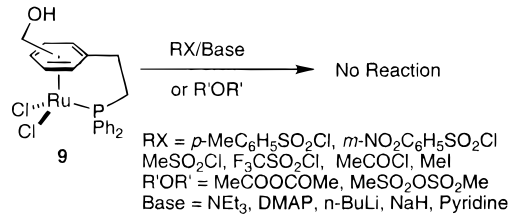

ylene protons unambiguously proves the coordination of the prochiral arene, yielding a racemic, planar chiral complex **9a**. The ^{1}H NMR (300 MHz) higher order ABCDX spin system arising from the diastereotopic CH_2CH_2P protons was simulated, and the resulting chemical shifts and coupling constants are listed in the Experimental Section. To our surprise, we were unable to functionalize the alcohol to a phosphinite or phosphite, albeit using many bases (including DBU, NEt_3, DMAP, NaH, *n*-BuLi, LDA, pyridine) in a wide range of solvents with various halophosphines namely: $ClP(Pyrrole)_2$, $ClPPh_2$, $ClP(OCH_2CH_2O)$, and $BrP(C_6F_5)_2$.

Despite the fact that the acidic O−H proton can be readily exchanged (as deduced from ^{1}H NMR H/D exchange experiments), it appears that benzylic alkoxide is totally inert toward P electrophiles. We, thus, studied the reactivity of **9a** toward C electrophiles. In the presence of a base, various acid chlorides and anhydrides (including tosyl, mesyl, acyl) did not react with **9a**. Eventually, we reasoned that the alkoxide may be a "soft nucleophile" and tested allylbromide, which is a soft electrophile. Again, no reaction was observed. In all cases, the starting material **9a** could be recovered in high yield after chromatography over silica gel (Scheme 3). To gain further insight, single crystals of **9a** were submitted for X-ray analysis. An ORTEP plot of the molecular structure of compound **9a** is presented in Figure 3. Relevant metrical data are collected in Table 3. From this data, we can exclude any direct intramolecular interaction between the oxygen and the ruthenium atoms. Even by artificially setting the O(1)−C(9)−C(2)−C(1) dihedral angle to −90°, thus minimizing the Ru−O distance, the oxygen remains too distant from the ruthenium (3.39 Å) to give rise to any significant bonding. From these observations, we reasoned that the alkoxide is sterically inaccessible. To avoid this problem, we synthesized the *meta* regioisomer **9b** (Scheme 4). The synthesis of the *meta*-hydroxyphosphine **4b** is very similar to the synthesis of its *ortho* analog **4a** (refer to Scheme 1). Phosphine coordination yielding **8b**, followed by arene displacement, affords **9b** in high yield. The reaction can be monitored by ^{31}P

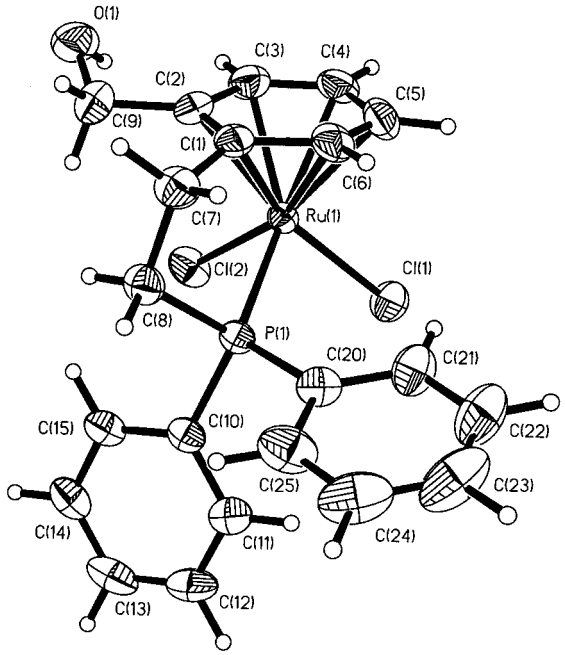

Figure 3. Molecular structure of [Ru(η^6:η^1-{*o*-(C_6H_4)(CH_2-OH)($CH_2CH_2PPh_2$)}Cl_2] (**9a**). Thermal ellipsoids are at the 50% probability level (solvent omitted for clarity).

Table 3. Selected Interatomic Distances (Å), Interatomic Angles (deg) and Torsion Angles (deg) for Compounds 9a and 9b

	9a	9b
Ru(1)−Cl(1)	2.4153(9)	2.4378(11)
Ru(1)−Cl(2)	2.3991(8)	2.4088(11)
Ru(1)−P(1)	2.3261(7)	2.3384(10)
Ru(1)−C(1)	2.166(3)	2.147(4)
Ru(1)−C(2)	2.200(3)	2.198(4)
Ru(1)−C(3)	2.224(3)	2.220(4)
Ru(1)−C(4)	2.255(3)	2.274(4)
Ru(1)−C(5)	2.196(3)	2.234(4)
Ru(1)−C(6)	2.199(3)	2.175(4)
O(1)−C(9)	1.403(5)	1.403(7)
C(2)−C(9)	1.510(5)	1.511(6)
Ru(1)−centroid	1.693(4)	1.695(4)
Ru(1)−O(1)	4.241(3)	3.761(4)
Cl(1)−Ru(1)−Cl(2)	86.56(3)	87.54(4)
Cl(1)−Ru(1)−P(1)	92.80(3)	93.90(4)
Cl(2)−Ru(1)−P(1)	88.70(3)	88.61(4)
O(1)−C(9)−C(2)	111.2(3)	114.6(4)
centroid−Ru(1)−Cl(1)	130.0(1)	128.4(1)
centroid−Ru(1)−Cl(2)	126.3(1)	126.4(1)
centroid−Ru(1)−P(1)	120.6(1)	120.8(1)
C(1)−C(7)−C(8)−P(1)	40.4(4)	−44.4(5)
O(1)−C(9)−C(2)−C(1)	157.4(3)	−34.2(7)[a]

[a] This dihedral angle corresponds to O(1)−C(9)−C(3)−C(2).

Scheme 4

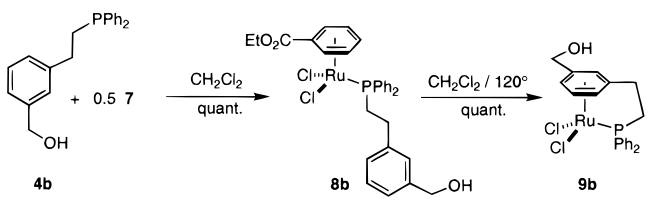

NMR spectroscopy as the P signal moves from −17.3 (compound **4b**) to 22.5 (compound **8b**) to 46.3 ppm (compound **9b**). Single crystals were grown, and the structure was determined by X-ray crystallography. An ORTEP plot of the molecular structure of compound **9b**

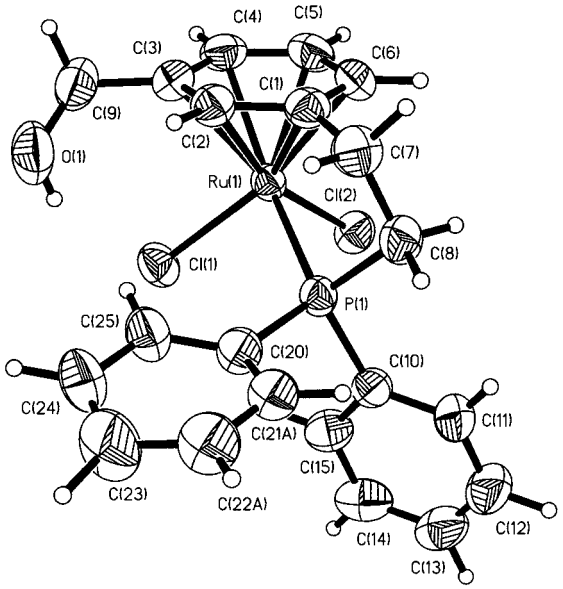

Figure 4. Molecular structure of $[Ru(\eta^6{:}\eta^1\text{-}\{m\text{-}(C_6H_4)(CH_2OH)(CH_2CH_2PPh_2)\}Cl_2]$ (**9b**). Thermal ellipsoids are at the 50% probability level (disorder and solvent omitted for clarity).

is presented in Figure 4. Relevant metrical data are collected in Table 3.

The reactivity of the benzylic alcohol **9b** toward nucleophiles was investigated (see Scheme 3). As for **9a**, all attempts to functionalize the alcohol were unsuccessful, yielding unreacted starting material **9b**, Scheme 3. Puzzled by the lack of reactivity of piano-stool complexes **9**, an extended Hückel (eH) analysis of the model $[Ru(\eta^6\text{-}C_6H_5CH_2O)(PH_3)Cl_2]^-$ was undertaken.

Extended Hückel Analysis. In order to understand the bonding in the model $[Ru(\eta^6\text{-}C_6H_5CH_2O)(PH_3)Cl_2]^-$, we constructed a simple three-legged piano-stool $[Ru(\eta^6\text{-}C_6H_6)H_3]^-$. Then we introduced the benzylic substituent on the arene, and finally, the hydrides were replaced by two chlorides capable of π-interaction and a model PH_3.

As a starting point, we recall the bonding between C_6H_6 and the C_{3v}-symmetric $\{RuH_3\}^-$ fragment.[38] A simplified interaction diagram is presented in Figure 5. The resulting "three below two" splitting pattern, reminiscent of octahedral coordination around ruthenium, is evident. With a d^6 electron count, the "t_{2g}" set, essentially located on the metal, is full.

Next, we substituted the benzene by a benzyl alkoxide $(C_6H_5CH_2O)^-$, setting the oxygen in the arene plane.[39] The oxygen orbitals hardly contribute (<2%) to the a_{2u}, e_{1g}, and e_{2u} arene FMOs, which are mostly responsible for the Ru−(η^6-arene) bonding. The approximate position of the oxygen "lone pair orbitals" is hatched in Figure 5.[40] As the Ru−O distance is too large to give

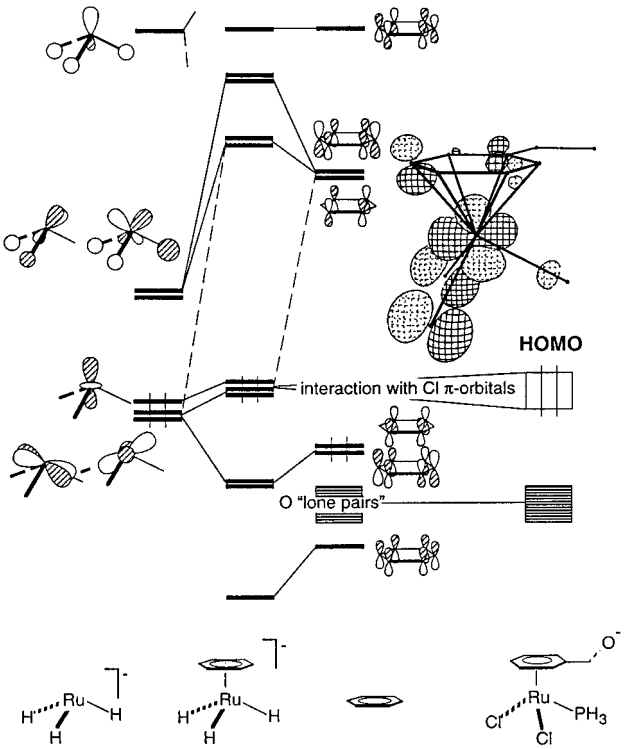

Figure 5. Qualitative interaction diagram for the model compounds $[Ru(\eta^6\text{-}C_6H_6)H_3]^-$ and $[Ru(\eta^6\text{-}C_6H_5CH_2O)(PH_3)Cl_2]^-$.

rise to an interaction, these orbitals remain unperturbed upon interaction between $(C_6H_5CH_2O)^-$ and $\{RuH_3\}^-$. As a consequence, the "t_{2g}" set of $[Ru(\eta^6\text{-}C_6H_5CH_2O)H_3]^{2-}$ contains no oxygen contribution (<2%). This leads to a significant negative charge build-up on the oxygen (-1.50 e$^-$).

Substituting the hydrides of $[Ru(\eta^6\text{-}C_6H_5CH_2O)H_3]^{2-}$ by two Cl's and a PH_3 group does not alter the picture much in $[Ru(\eta^6\text{-}C_6H_5CH_2O)PH_3Cl_2]^-$. The Ru−Cl π interactions slightly destabilize the corresponding Ru "t_{2g}" orbitals, which remain essentially Ru−arene nonbonding. Each Cl ligand contributes ~10% to each MO in the "t_{2g}" set. The HOMO is depicted on the right of Figure 5. The net atomic charges are distributed as follow: Ru, +0.49 e$^-$; Cl, −0.57 e$^-$; O, −1.50 e$^-$; C_{benzyl}, +0.45 e$^-$.

For a frontier-orbital-controlled reaction on $[Ru(\eta^6\text{-}C_6H_5CH_2O)PH_3Cl_2]^-$, an incoming electrophile should not interact with the oxygen as it does not contribute to the highest lying occupied orbitals. If the reaction is charge-controlled, however, the electrostatic interaction will favor attack on the oxygen as it bears the greatest negative charge. Recently, Weber *et al.* have implemented a formalism to evaluate from eH calculations the intermolecular interaction energy E_{int} between an organometallic substrate **S** and a model electrophilic or nucleophilic reagent **R**.[41] In addition to the electrostatic part,[41,42] charge-transfer[43] and exchange-repulsion[44] components have been included in the calculation of a

(38) Albright, T. A.; Burdett, J. K.; Whangbo, M.-H. *Orbital Interactions in Chemistry*; John Wiley: New York, 1985.

(39) Setting the oxygen in the arene plane yields a hyperconjugated oxygen lone pair, ensuring a maximal contribution of the oxygen orbitals to the π-system of the coordinated arene. Variation of the $O-CH_2-C_{ipso}-C_{Ar}$ dihedral angle to match the structurally determined angles in **9a** or **9b** affords even smaller contributions of the lone pairs to the π-system.

(40) By oxygen "lone-pair" we mean orbitals with a significant contribution (>30%) of the oxygen atomic orbitals.

(41) Weber, J.; Stussi, D.; Fluekiger, P.; Morgantini, P.-Y. *Comm. Inorg. Chem.* **1992**, *14*, 27.

(42) Scrocco, E.; Tomasi, J. *Top. Curr. Chem.* **1973**, *42*, 95.

(43) Brown, D. A.; Fitzpatrick, N. J.; McGinn, M. A. *J. Organomet. Chem.* **1985**, *293*, 235.

(44) Weber, J.; Flueckiger, P.; Stussi, D.; Morgantini, P.-Y. *J. Mol. Struct. (Theochem)* **1992**, *221*, 175.

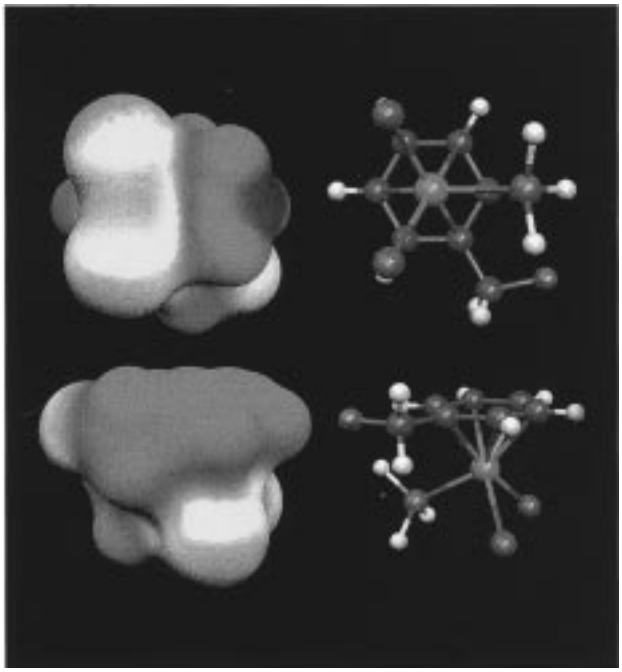

Figure 6. Solvent-accessible surface for $[Ru(\eta^6\text{-}C_6H_5\text{-}CH_2O)(PH_3)Cl_2]^-$, shaded according to the E_{int} value for electrophilic attack (red-shaded, most reactive; blue-shaded, least reactive).

local reactivity index to interpret and predict the regio- and stereoselectivity of electrophilic and nucleophilic addition reactions to organometallics. The solvent-accessible surface of the substrate, generated using the method suggested by Connolly,[45] is used for representing the intermolecular interaction energies E_{int} encoded by color. The most reactive sites are red-shaded, while the least reactive sites are blue-shaded. The results of the nucleophilicity index computations for $[Ru(\eta^6\text{-}C_6H_5\text{-}CH_2O)PH_3Cl_2]^-$ can be visualized in Figure 6. From this figure, it is immediately apparent that the most nucleophilic region is located between the chlorides. This can be rationalized by the fact that the chlorides bear a significant negative charge *and* contribute to the HOMO, thus favoring both frontier-orbital- and charge-controlled attack.

X-ray Data. All four structurally characterized compounds **6a**, **7**, **9a**, and **9b** (see Table 4 for a summary of crystallographic data) were compared with related X-ray crystal structures retrieved from the Cambridge Structural Database (CSD). To our knowledge, only one ruthenium edge-bridged chloro−arene dimer has been structurally characterized: $[Ru(\eta^6\text{-}Me_6C_6)Cl_2]_2$.[46] The data for $[Ru(\eta^6\text{-}EtO_2CC_6H_5)Cl_2]_2$ (**7**) is very similar. Fourteen structures incorporating the $[Ru(\eta^6\text{-arene})(P\text{-donor})Cl_2]$ motif were retrieved from the CSD.[47] Again, all bond lengths and angles for compounds **6a**, **9a**, and **9b** are comparable. Perhaps worth noting is the Ru−(η^6-arene) distance which does not vary significantly from **6a** (1.704(7) Å) to the phosphine-tethered **9a** (1.693(4) Å) and **9b** (1.695(4) Å). The dihedral angles C(1)−C(7)−C(8)−P(1) for **9a** (40.4(4)°) and **9b** (44.4(5)°) indicate that the structure is staggered rather than eclipsed. For all structurally characterized complexes, **6a**, **7**, **9a**, and **9b**, the coordinated η^6-arene remains essentially planar, although incorporation of the phosphine tether tends to force the *ipso* carbon toward the metal center (maximum out of plane C(5) = −0.027 Å, C(6) = 0.027 Å for **9a**; C(2) = 0.024 Å, C(3) = −0.024 Å for **9b**).[29] For regioisomers **9a** and **9b**, the oxygen points away from (O(1)−C(9)−C(2)−C(1) = 157.4(3)°) and toward (O(1)−C(9)−C(3)−C(2) = −34.3(7)°) the ruthenium, respectively, thus setting the oxygen at 4.241(3) and 3.761(4) Å from the metal, respectively.

Outlook. We have developed a straightforward synthesis of racemic, planar chiral $[Ru(\eta^6\text{:}\eta^1\text{-}C_6H_4(CH_2OH)(CH_2CH_2PPh_2))Cl_2]$ complexes. Despite intensive efforts, the alcohol could not be functionalized by various electrophiles. This lack of reactivity can be rationalized by eH calculations: the absence of oxygen contributions in the highest lying occupied molecular orbitals does not favor attack at this position, despite a high negative charge located on the oxygen. Recently, Ganter *et al.* reported the synthesis of a series of substituted phosphaferrocenes **10**.[48] Interestingly, the phosphinite **10b**

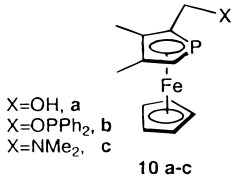

10 a-c

could only be prepared in very low yield from the corresponding alcohol **10a**. We believe that the reason for this can be traced back to similar orbital arguments as those presented above. Our attempts to synthesize complexes of type **1** via a different route will be reported in due time.

Experimental Section

General Considerations. NMR spectra were recorded on either a Varian XL 200 (^{31}P), Brucker AM 300 (^{1}H), or Bruker DRX 400 (^{19}F) spectrometer. Chemical shifts are given in parts per million (ppm) and coupling constants in hertz. Signals are referenced against H_3PO_4 (^{31}P, external reference), $CFCl_3$ (^{19}F, external reference), and tetramethylsilane (^{1}H, internal reference). Combustion analyses were carried out by Novartis, Basel. Except for $RuCl_3 \cdot xH_2O$ (Johnson Matthey), all chemicals were purchased either from Fluka AG or from Aldrich. Silica gel was used for flash chromatography (Fluka, silica gel 60). All reactions were carried out under Schlenk conditions, and all solvents were distilled under nitrogen with standard desiccating agents. The following compounds were prepared as described elsewhere: ethyl-1,4-cyclohexadiene-3-carboxylate,[35] 2-vinylbenzaldehyde (**2a**),[49] 3-vinylbenzaldehyde (**2b**),[50] bis(pentafluorophenyl)bromophosphine,[31] $[RuCl_2(p\text{-cymene})]_2$.[34]

Structure Determination. X-ray diffraction data were collected on a Siemens SMART CCD diffractometer[51] at room temperature using monochromated graphite Mo Kα radiation

(45) Connolly, M. L. Molecular Surface Program. *QCPE Bull. 1 74*, 1981.
(46) McCormick, F. B.; Gleason, W. B. *Acta Crystallogr., Sect. C* **1988**, *44*, 603.
(47) CSD refcodes for $[Ru(\eta^6\text{-arene})(P\text{-donor})Cl_2]$ complexes: BUWHEG, BYRUMP, CMRUMP, FALKEY, FUBNOF, GAPZEB, GAPZIF, KATGOB, KOFYEK, LASGER, LESTOS, LIFSUO, PILHIB, ZESSAR.
(48) Ganter, C.; Brassat, L.; Glinsböckel, C.; Ganter, B. *Organometallics* **1997**, *16*, 2862.
(49) Hartman, G. D.; Halczenko, W.; Phillips, B. T. *J. Org. Chem.* **1985**, *50*, 2427.
(50) Hirao, A.; Kitamura, K.; Takenaka, K.; Nakahama, S. *Macromolecules* **1993**, *26*, 4995.
(51) *SMART, version 4. Software for the CCD Detector system*; Siemens Analytical Instruments Division: Madison, WI, 1995.

Table 4. Summary of Crystallographic Data for Compounds 6a, 7, 9a, and 9b

	6a	7	9a	9b
formula	$C_{31}H_{35}Cl_2OPRu$	$C_{18}H_{20}Cl_4O_4Ru_2$	$C_{22}H_{23}Cl_4OPRu$	$C_{22}H_{23}Cl_4OPRu{\cdot}CH_2Cl_2$
fw	626.53	644.28	577.24	662.17
cryst syst	triclinic	monoclinic	orthorhombic	triclinic
space group	$P\bar{1}$	$P2_1/c$	$P2_12_12_1$	$P\bar{1}$
a, Å	12.5570(1)	11.9235(9)	7.3833(4)	9.4413(8)
b, Å	15.5708(3)	6.9971(5)	12.9998(7)	11.2840(9)
c, Å	16.2025(3)	13.814(1)	24.097(1)	11.612(1)
α, deg	67.662(1)			84.967(1)
β, deg	78.023(1)	110.023(1)		79.061(1)
γ, deg	89.698(1)			72.286(1)
V, Å^3	2856.94(8)	1082.8(1)	2312.9(2)	1156.4(2)
Z	4	2	4	2
ρ_{calcd}, mg/m^3	1.457	1.976	1.658	1.658
μ, mm^{-1}	0.814	1.910	1.221	1.221
F(000)	1288	632	1160	576
cryst size, mm	0.24 × 0.20 × 0.14	0.15 × 0.06 × 0.02	0.20 × 0.20 × 0.20	0.22 × 0.22 × 0.09
T, K	298(2)	298(2)	298(2)	298(2)
exposure time, sec	10	40	10	10
scan range, deg	$1.39 < \theta < 23.24$	$1.82 < \theta < 26.39$	$1.69 < \theta < 26.38$	$1.79 < \theta < 23.28$
total no. of data	12002	5000	11557	7152
no. of unique obsd data	8067	2020	4339	3300
no. of variables	725	131	266	273
goodness-of-fit	1.160	1.141	1.060	1.052
R(int)	0.0321	0.0275	0.0437	0.0537
final R_1[a] [$I > 2\sigma(I)$]	0.0465	0.0261	0.0253	0.0349
final wR_2[b] (all data)	0.0977	0.0561	0.0617	0.0928
max, min resid density, e Å^{-3}	0.481, −0.415	0.355, −0.424	0.503, −0.407	0.692, −0.658

[a] $R_1 = \sum||F_o| - |F_c||/\sum|F_o|$. [b] $wR_2(F_o^2) = \{\sum[w(F_o^2 - F_c^2)^2]/\sum[w(F_o^2)]\}$; $w = 1/[\sigma^2(F_o^2) + P^2 + P]$, where $P = (F_o^2 + 2F_c^2)/3$.

(0.710 73 Å) The relevant structure determination parameters are given in Table 4. A complete hemisphere of data was scanned on ω (0.30) with a run time of 10 or 40 s unless otherwise stated) at the detector resolution of 512 × 512 pixels and a detector distance of 5.18 cm. A total of 1271 frames were collected for each data set. Cell constants were obtained on 60 frames. The collected frames were processed with the SAINT program[52] that automatically performs Lorentz and polarization corrections. Empirical absorption corrections were made using the XPREP program from the SHELXTL[53] software. The structures were solved by direct methods, and the refinement was done by full-matrix least-squares of F^2 using SHELXL96[54] (beta-test version). All non-hydrogen atoms were refined anisotropically, while hydrogen atoms, included at calculated positions, were refined in the riding model with group atomic displacement parameters.

Synthesis of *o*-$C_6H_4(CHO)(CH_2CH_2PPh_2)$ (3a). A degassed, diethyl ether solution (15 mL) containing diphenylphosphine (6.34 g, 34.1 mmol), styrene (**2a**) (4.50 g, 34.1 mmol), and AIBN (0.28 g, 1.7 mmol) was irradiated (Hg low-pressure lamp) in a sealed Schlenk flask for 24 h. The volatile materials were removed *in vacuo*. The phosphine **3a** proved to be pure (>95%) by NMR and was used without purification. ^{1}H NMR ($CDCl_3$): 10.10 (s, 1H, C**H**O), 7.6−7.1 (m, 14H, C_{Ar}**H**), 2.94 (dt, $^3J_{H-H}$ = 8.5 Hz, $^2J_{H-P}$ = 7.5 Hz, 2H, C$\mathbf{H}_2$P), 2.42 (t, 2H, $C_{Ar}C\mathbf{H}_2$). ^{31}P NMR ($CDCl_3$): −16.1.

Synthesis of *m*-$C_6H_4(CHO)(CH_2CH_2PPh_2)$ (3b). This compound was prepared similarly to its *ortho*-regioisomer **3a**, starting from 2.80 g (21.2 mmol) of 3-vinylbenzaldehyde (**2b**).^{1}H NMR ($CDCl_3$): 10.10 (s, 1H, C**H**O), 7.6−7.0 (m, 14H, C_{Ar}**H**), 2.80 (m, 2H, C$\mathbf{H}_2$P), 2.50 (m, 2H, $C_{Ar}C\mathbf{H}_2$). ^{31}P NMR ($CDCl_3$): −17.3.

Synthesis of *o*-$C_6H_4(CH_2OH)(CH_2CH_2PPh_2)$ (4a). A benzene−ethanol mixture (5:1) was charged with **3a** (10.84 g, 34.1 mmol), degassed, and cooled to 0 °C. $NaBH_4$ (1.33 g, 35.0 mmol) was added portionwise. The mixture was then allowed to slowly warm to room temperature and stirred for 4 h. The solution was then acidified with HCl (5% solution). The organic layer was separated, and the aqueous layer was extracted with diethyl ether. The combined organic phases were washed with water, dried over $MgSO_4$, and concentrated under vacuum. The product was purified by flash chromatography (hexane/EtOAc gradient 5:1 to 1:1), affording the phosphino−alcohol **4a** in 85% yield (9.28 g, 29.0 mmol). ^{1}H NMR ($CDCl_3$): 7.7−7.1 (m, 14H, C_{Ar}**H**), 4.58 (s, 2H, C$\mathbf{H}_2$O), 2.81 (dt, $^3J_{H-H}$ = 8.5 Hz, $^2J_{H-P}$ = 7.0 Hz, 2H, C$\mathbf{H}_2$P), 2.37 (t, 2H, $C_{Ar}C\mathbf{H}_2$), 1.60 (brd, 1H, O**H**). ^{31}P NMR ($CDCl_3$): −15.8. Anal. Calcd for $C_{21}H_{20}OP{\cdot}0.4H_2O$: C, 77.24; H, 6.42. Found: C, 77.5; H, 6.2.

Synthesis of *m*-$C_6H_4(CH_2OH)(CH_2CH_2PPh_2)$ (4b). This compound was prepared similarly to its regioisomer **4a**. The product was purified by flash chromatography (hexane/EtOAc 9:1), affording the phosphino alcohol **4b** in 78% yield (5.32 g, 16.6 mmol). ^{1}H NMR ($CDCl_3$): 7.52 (m, 4H, C_{Ar}**H**), 7.38 (m, 6H, C_{Ar}**H**), 7.26 (dd, $^3J_{H-H}$ = 7.4 Hz, $^3J_{H-H}$ = 7.4 Hz, 1H, C_{Ar}**H**), 7.24 (s, 1H, C_{Ar}**H**), 7.18 (d, 1H, C_{Ar}**H**), 7.10 (d, 1H, C_{Ar}**H**), 4.67 (s, 2H, C$\mathbf{H}_2$O), 2.79 (dt, $^3J_{H-H}$ = 8.5 Hz, $^2J_{H-P}$ = 8.7 Hz, 2H, C$\mathbf{H}_2$P), 2.48 (t, 2H, $C_{Ar}C\mathbf{H}_2$), 2.3 (brd, 1H, O**H**). ^{31}P NMR ($CDCl_3$): −17.3. Anal. Calcd for $C_{21}H_{20}OP{\cdot}0.2H_2O$: C, 78.10; H, 6.37. Found: C, 78.2; H, 6.2.

Synthesis of *o*-$C_6H_4(CH_2OP(C_6F_5)_2)(CH_2CH_2PPh_2)$ (5a). To a stirred solution of phosphino−alcohol **4a** (1.19 g, 3.71 mmol) in diethyl ether containing triethylamine (5.1 mL, 37 mmol), bis(pentafluorophenyl)bromophosphine (1.66 g, 3.71 mmol) was slowly added by means of a syringe. After 24 h at room temperature, the suspension was filtered and the volatiles were evaporated *in vacuo*. Flash chromatography with hexane:ethyl acetate (1:1) yields phosphino phosphinite **5a** in 38% yield (958 mg, 1.4 mmol). ^{1}H NMR ($CDCl_3$): 7.7−7.1 (m, 14H, C_{Ar}H), 4.87 (d, $^3J_{H-P}$ = 11.8 Hz, 2H, C$\mathbf{H}_2$O), 2.73 (m, 2H, C$\mathbf{H}_2$P), 2.27 (m, 2H, $C_{Ar}C\mathbf{H}_2$). ^{31}P NMR ($CDCl_3$): −16.2 (s, 1P), 87.6 (quin, $^3J_{F-P}$ = 34 Hz, 1P). ^{19}F NMR ($CDCl_3$) −6.14 (tm, $^3J_{F-P}$ = 34 Hz, $^3J_{F-F}$ = 18.3 Hz, $^4J_{F-F}$ = 3.8 Hz, 4F), −22.34 (tt, $^3J_{F-F}$ = 20.4 Hz, 2F), −33.49 (tm, $^4J_{F-P}$ = 1.8 Hz, 4F).

(52) *SAINT, version 4*; Siemens Energy and Automation Inc.: Madison, WI, 1995.
(53) *SHELXTL, version 5.03 (for Silicon Graphics). Program Library for Structure Solution and Molecular Graphics*; Siemens Analytical Instruments Division: Madison, WI, 1995.
(54) Sheldrick, G. M. *SHELXL-96; Program for the Refinement of Crystal Structures;* University of Göttingen: Göttingen, Germany, 1996.

Synthesis of [Ru(η^6-*p*-cymene)(η^1-*o*-$C_6H_4(CH_2OH)$-$(CH_2CH_2PPh_2)$)Cl_2] (6a). $[RuCl_2(p\text{-cymene})]_2$ (0.20 g, 0.33 mmol) and phosphino alcohol **4a** (0.210 g, 0.65 mmol) were dissolved in dichloromethane (10 mL), and the mixture was stirred for 30 min. Addition of benzene (250 mL) yields a brownish microcrystalline product **6a** (375 mg, 0.60 mmol, 92% yield). The air-stable solid is placed in a Soxhlet extractor and extracted under nitrogen with isopropanol alcohol, affording red crystals suitable for X-ray analysis. ^{1}H NMR ($CDCl_3$): 7.93 (m, 4H, C_{Ar}**H**), 7.53 (m, 6H, C_{Ar}**H**), 7.23 (dd, $^3J_{H-H}$ = 4.4 Hz, $^4J_{H-H}$ = 1.5 Hz, 1H, C_{Ar}**H**), 7.08 (m, 2H, C_{Ar}**H**), 6.87 (dd, 1H, C_{Ar}**H**), 5.29 (d, $^3J_{H-H}$ = 5.9 Hz, 2H, C_{cym}**H**), 5.10 (d, 2H, C_{cym}**H**), 4.46 (d, $^3J_{H-H}$ = 5.5 Hz, 2H, C**H**$_2$O), 2.80 (td, 2H, $^3J_{H-H}$ = 9.1 Hz, $^2J_{H-P}$ = 9.2 Hz, C**H**$_2$P), 2.56 (sep, $^3J_{H-H}$ = 7.0 Hz, 1H, C**H**$(CH_3)_2$), 2.46 (dt, $^3J_{H-P}$ = 4.4 Hz, 2H, C_{Ar}C**H**$_2$), 2.22 (t, 1H, O**H**), 1.91 (s, 3H, C_{Ar}C**H**$_3$), 0.88 (d, 6H, CH(C**H**$_3$)$_2$). ^{31}P NMR ($CDCl_3$): 20.2. Anal. Calcd for $C_{31}H_{35}Cl_2OPRu\cdot 0.33C_6H_6$): C, 60.74; H, 5.71. Found: C, 60.8; H, 5.6.

Synthesis of $[RuCl_2(EtO_2CC_6H_5)]_2$ (7). This complex was prepared by an analogous method to that used for $[RuCl_2(C_6H_6)]_2$.[34] A solution of $RuCl_3\cdot 3H_2O$ (3.85 g, 14.7 mmol) and 4 equiv of ethyl-1,4-cyclohexadiene-3-carboxylate (8.50 g, 55.8 mmol) in ethanol was refluxed for 12 h. The orange, air-stable, microcrystalline material (4.59 g, 96% yield) was then placed in a Soxhlet extractor and extracted under nitrogen with ethanol, affording red crystals suitable for X-ray analysis. ^{1}H NMR ($CDCl_3$): 6.48 (d, $^3J_{H-H}$ = 5.6 Hz, 4H, C_{Ar}**H**), 5.99 (t, $^3J_{H-H}$ = 5.6 Hz, 2H, C_{Ar}**H**), 5.79 (dd, 4H, C_{Ar}**H**), 4.45 (q, $^3J_{H-H}$ = 7.0 Hz, 4H, OC**H**$_2$), 1.40 (t, 6H, C**H**$_3$). Anal. Calcd for $C_9H_{10}Cl_2O_2Ru$: C, 33.56; H, 3.13. Found: C, 33.5; H, 3.1.

Synthesis of [Ru(η^6-$C_6H_5CO_2Et$)(η^1-*o*-$C_6H_4(CH_2OH)$-$(CH_2CH_2PPh_2)$)Cl_2] (8a). To a dichloromethane solution (20 mL) of dimer **7** (0.406 g, 0.63 mmol), phosphino alcohol **4a** (380 mg, 1.19 mmol) was added. The mixture was stirred for 30 min. The solid was precipitated with hexane to give **8a** in 98% yield (0.746 g, 1.17 mmol). ^{1}H NMR ($CDCl_3$): 7.9 (m, 4H, C_{Ar}**H**), 7.5 (m, 6H, C_{Ar}**H**), 7.3 (m, 1H, C_{Ar}**H**), 7.10 (m, 2H, C_{Ar}**H**), 6.92 (m, 1H, C_{Ar}**H**), 6.34 (d, $^3J_{H-H}$ = 5.6 Hz, 2H, C_{ester}**H**), 5.44 (t, $^3J_{H-H}$ = 5.6 Hz, 1H, C_{ester}**H**), 5.10 (dd, 2H, C_{ester}**H**), 4.51 (s, 2H, C**H**$_2$OH), 4.37 (q, $^3J_{H-H}$ = 7.0 Hz, 2H, OC**H**$_2$), 2.88 (m, 2H, C**H**$_2$P), 2.56 (m, 2H, C_{Ar}C**H**$_2$), 1.39 (t, 3H, C**H**$_3$). ^{31}P NMR ($CDCl_3$): 21.8. Anal. Calcd for $C_{30}H_{31}Cl_2O_3PRu$: C, 56.08; H, 4.86. Found: C, 55.7; H, 4.9.

Synthesis of [Ru(η^6-$C_6H_5CO_2Et$)(η^1-*m*-$C_6H_4(CH_2OH)$-$(CH_2CH_2PPh_2)$)Cl_2] (8b). To a dichloromethane solution (15 mL) of dimer **7** (0.241 g, 0.37 mmol), phosphino alcohol **4b** (250 mg, 0.78 mmol) was added. The mixture was stirred for 20 min. The volume was reduced to 5 mL. Then the orange solid was precipitated with diethyl ether (500 ml) to give **8b** in 93% yield (0.450 g, 0.70 mmol). ^{1}H NMR (acetone-d_6): 8.00 (m, 4H, C_{Ar}**H**), 7.56 (m, 6H, C_{Ar}**H**), 7.15 (m, 2H, C_{Ar}**H**), 7.02 (s, 1H, C_{Ar}**H**), 6.90 (d, $^3J_{H-H}$ = 6.6 Hz, 1H, C_{Ar}**H**), 6.33 (d, $^3J_{H-H}$ = 6.3 Hz, 2H, C_{ester}**H**), 5.66 (m, 1H, C_{ester}**H**), 5.22 (dd, $^3J_{H-H}$ = 5.7 Hz, 2H, C_{ester}**H**), 4.52 (d, $^3J_{H-H}$ = 5.5 Hz, 2H, C**H**$_2$OH), 4.35 (q, $^3J_{H-H}$ = 7.0 Hz, 2H, OC**H**$_2$), 4.10 (t, 1H, O**H**), 2.88 (m, 2H, C**H**$_2$P), 2.47 (m, 2H, C_{Ar}C**H**$_2$), 1.32 (t, 3H, C**H**$_3$). ^{31}P NMR (acetone-d_6): 22.5. Anal. Calcd for $C_{30}H_{31}Cl_2O_3PRu$: C, 56.08; H, 4.86; Cl, 11.04. Found: C, 56.1; H, 4.9; Cl, 11.1.

Synthesis of [Ru(η^6:η^1-*o*-$C_6H_4(CH_2OH)(CH_2CH_2PPh_2)$)-$Cl_2$] (9a). A 25 mL pressure Schlenk tube was charged with dichloromethane (8 mL), Ru dimer **7** (0.472 g, 0.73 mmol), and phosphino alcohol **4a** (0.469 g, 1.47 mmol). After 3 freeze−pump−thaw cycles, the mixture was heated at 120 °C for 24 h and cooled to room temperature, and the product was precipitated with hexane (200 mL). The orange solid was filtered, washed with ether, and dried *in vacuo* to give 0.703 g (1.43 mmol) of **9a**, 97% yield. Suitable crystals for X-ray diffraction of **9a** were obtained by slow evaporation of a saturated solution in dichloromethane. ^{1}H NMR ($CDCl_3$): 8.03 (m, 2H, PC_{Ar}**H**), 7.55 (m, 2H, C_{Ar}**H**), 7.47 (m, 3H, C_{Ar}**H**), 7.33 (m, 3H, C_{Ar}**H**), 6.59 (d, $^3J_{H-H}$ = 6.6 Hz, 1H, η^6-$C_{Ar\alpha}$**H**), 6.30 (brd t, $^3J_{H-H}$ = 5.5 Hz, $^4J_{H-H}$ = 2.4 Hz, 1H, η^6-$C_{Ar\beta}$**H**), 5.59 (dd, $^3J_{H-H}$ = 5.5 Hz, 1H, η^6-$C_{Ar\delta}$**H**), 5.00 (dd, 1H, η^6-$C_{Ar\gamma}$**H**), 4.67 (dd, $^2J_{H-H}$ = 14.0 Hz, $^3J_{H-H}$ =8.1 Hz, 1H, C**H**HO), 4.52 (dd, $^3J_{H-H}$ = 5.1 Hz, 1H, C**H**HO), 4.22 (dd, 1H, O**H**), 3.92 (m, $^2J_{A-B}$ = 14.0 Hz, J_{A-C} = 8.8 Hz, $^3J_{A-D}$ = 2.9 Hz, $^3J_{A-X}$ = 17.3 Hz, 1H, C**H**$_A$HP), 3.81 (m, $^3J_{B-C}$ = 1.8 Hz, $^3J_{B-D}$ = 6.3 Hz, $^3J_{B-X}$ = 14.3 Hz, 1H, CH**H**$_B$P), 2.88 (m, $^2J_{C-D}$ = 16.0 Hz, $^4J_{C-X}$ = 34.4 Hz, 1H, C_{Ar}C**H**$_C$H), 2.58 (m, $^4J_{D-X}$ = 10.5 Hz, 1H, C_{Ar}-CH**H**$_D$) (ABCDX spin-system simulated). ^{31}P NMR ($CDCl_3$): 41.5. Anal. Calcd for $C_{21}H_{21}Cl_2OPRu$: C, 51.23; H, 4.30; Cl, 14.40. Found: C, 50.9; H, 4.3; Cl, 14.2.

Synthesis of [Ru(η^6:η^1-*o*-$C_6H_4(CH_2OH)(CH_2CH_2PPh_2)$)-$Cl_2$] (9b). A 25 mL pressure Schlenk tube was charged with dichloromethane (10 mL) and **8b** (0.405 g, 0.63 mmol). After 3 freeze−pump−thaw cycles, the mixture was heated at 120 °C for 24 h and cooled to room temperature, and the product was precipitated with hexane (200 mL). The orange solid was filtered, washed with ether and purified by flash chromatography (EtOAc), affording **9b** in 65% yield (200 mg, 0.41 mmol). Suitable crystals for X-ray diffraction of **9b** were obtained by slow evaporation of a saturated solution in dichloromethane. ^{1}H NMR ($CDCl_3$): 7.71 (m, 4H, C_{Ar}**H**), 7.40 (m, 6H, C_{Ar}**H**), 6.28 (d, $^3J_{H-H}$ = 6.1 Hz, 1H, η^6-$C_{Ar\alpha}$**H**), 6.07 (dd, $^3J_{H-H}$ = 5.5 Hz, 1H, η^6-$C_{Ar\beta}$**H**), 5.11 (s, 1H, η^6-C_{Ar}**H**), 5.03 (d, $^3J_{H-H}$ = 5.5 Hz, 1H, η^6-$C_{Ar\delta}$**H**), 4.72 (dd, $^2J_{H-H}$ = 15.1 Hz, $^3J_{H-H}$ = 7.4 Hz, 1H, C**H**HO), 4.55 (dd, $^3J_{H-H}$ = 7.4 Hz, 1H, CH**H**O), 4.18 (dd, 1H, O**H**), 3.50 (m, 2H, C**H**$_2$P), 2.66 (m, 2H, C_{Ar}C**H**$_2$). ^{31}P NMR ($CDCl_3$): 46.3. Anal. Calcd for $C_{21}H_{21}Cl_2OPRu\cdot 1.5CH_2Cl_2$: C, 43.6; H, 3.9. Found: C, 43.3; H, 3.8.

Acknowledgment. T.R.W. thanks Prof. A. Ludi for his hopsitality, Prof H.-B. Bürgi for stimulating discussions and diffractometer time, the Swiss National Science Foundation for funding, and the *Stiftung für Stipendien auf dem Gebiete der Chemie* for the award of a Werner Fellowship (1994−1998).

Appendix

The eH calculations were performed with the CACAO package, using standard parameters.[55−58] All distances and angles for the model calculations were taken from the X-ray structure of **9a**, except for Ru−H = 1.7 Å. All eH parameters were taken from ref 24. The reactivity index calculations[41] were carried out with the modified eH procedure to include core−core repulsion as formulated by Calzaferri.[59]

Supporting Information Available: Tables of crystal data, atomic coordinates, anisotropic thermal parameters, bond lengths, and bond angles of **6a**, **7**, **9a**, and **9b** (16 pages). Ordering information is given on any current masthead page.

OM970735L

(55) Ammeter, J. H.; Bürgi, H.-B.; Thibeault, J. C.; Hoffmann, R. *J. Am. Chem. Soc.* **1978**, *100*, 3686.
(56) Hoffmann, R.; Lipscomb, W. N. *J. Chem. Phys.* **1962**, *36*, 2179.
(57) Hoffmann, R. *J. Chem Phys.* **1963**, *39*, 1397.
(58) Mealli, C.; Proserpio, D. M. *J. Chem. Educ.* **1990**, *67*, 399.
(59) Calzaferri, G.; Brändle, M. ICON & INPUTC. QCPE No. 116.